ANNUAL PROGRESS REPORT

INVESTIGATION OF PLASMA INSTABILITIES IN THE POLAR CUSP

For the Period:

1 September 1993 through 28 February 1994

Principal Investigator:

H.K. Wong
Southwest Research Institute
Department of Space Sciences
P.O. Drawer 28510
San Antonio, TX 78228-0510

SwRI Project 15-2779

NASA Grant No. NAGW-1620

Electron Beam Excitation of Upstream Waves in the Whistler Mode Frequency Range

Hung K. Wong
Department of Space Sciences, Southwest Research Institute, San Antonio, Texas

and

Charles W. Smith
Bartol Research Institute, University of Delaware, Newark, Delaware

Submitted to the Journal of Geophysical Research on October 8, 1993.

Revised and resubmitted on February 11, 1994.

Abstract. We examine whistler mode instabilities arising from electron beams in interplanetary space at 1 AU. Both parallel and obliquely propagating solutions are considered. We demonstrate that the generation of two simultaneous whistler mode waves is possible, and even reasonably likely, for beam parameters frequently encountered upstream of the Earth's bow shock and at interplanetary shocks. We also explore the generation of left-hand polarized waves at whistler mode frequencies under these same conditions. We offer both parametric variations derived from numerical solutions of the various instabilities as well as an analytical treatment of the problem which succeeds in unifying the various numerical results.

I. PROGRESS TO DATE

During the last six months, we have made considerable progress in studying the excitation of electromagnetic waves in the whistler frequency range by an anisotropic or gyrating electron beam. A paper entitled "Electron Cyclotron Wave Generation by Relativistic Electrons" was published in the Journal of Geophysical Research. Another paper entitled "Electron Beam Excitation of Upstream Waves in the Whistler Mode Frequency Range" was submitted for publication in Journal of Geophysical Research. This paper is in collaboration with Dr. C. W. Smith at Bartol Research Institute. In this paper, we have shown that an anisotropic electron beam (or gyrating electron beam) is capable of generating both left-hand and right-hand polarized electromagnetic waves in the whistler frequency range.

Our earlier paper "Electromagnetic Components of Auroral Hiss and Lower Hybrid Waves in the Polar Magnetosphere" was accepted for publication in the AGU Chapman Conference on Micro and Meso Scale Phenomena in Space Plasmas. This paper identified electromagnetic waves in the lower hybrid and whistler waves regime and suggested a mechanism of how these waves are generated.

II. CURRENT WORK

We are currently studying how the variation of the background plasma and the anisotropic beam parameters can affect the beam excited electromagnetic whistler instability. Our preliminary analytical results indicated that even an isotropic electron beam can excite electromagnetic whistler waves via cyclotron resonance in a high density plasma in which the electron plasma frequency is above the electron cyclotron frequency. This is quite different from the conventional thinking that electron beam can only excite whistler waves through Landau resonance, thus the excited waves have to be predominately electrostatic in nature. We are also in the process of studying the acceleration of electrons and ions by electromagnetic whistler and lower hybrid waves in the auroral region. This work is in collaboration with Drs. J. D. Menietti and C. S. Lin and the results will be presented in the Spring AGU meeting.

JOURNAL OF GEOPHYSICAL RESEARCH, VOL. 99, NO. A1, PAGES 235–239, JANUARY 1, 1994

Electron cyclotron wave generation by relativistic electrons

H. K. Wong
Department of Space Sciences, Southwest Research Institute, San Antonio, Texas

M. L. Goldstein
Laboratory of Extraterrestrial Physics, NASA Goddard Space Flight Center, Greenbelt, Maryland

Abstract. We show that an energetic electron distribution which has a temperature anisotropy ($T_{\perp b} > T_{\parallel b}$), or which is gyrating about a DC magnetic field, can generate electron cyclotron waves with frequencies below the electron cyclotron frequency. Relativistic effects are included in solving the dispersion equation and are shown to be quantitatively important. The basic idea of the mechanism is the coupling of the beam mode to slow waves. The unstable electron cyclotron waves are predominantly electromagnetic and right-hand polarized. For a low-density plasma in which the electron plasma frequency is less than the electron cyclotron frequency, the excited waves can have frequencies above or below the electron plasma frequency, depending upon the parameters of the energetic electron distribution. This instability may account for observed Z mode waves in the polar magnetosphere of the Earth and other planets.

Introduction

The Earth's polar magnetosphere has long been recognized as an active region of wave activities. In the last two decades, numerous spacecraft have sampled this region of space and have identified a large variety of wave modes, most notably the auroral hiss and the auroral kilometric radiation (AKR). For a review, see *Shawhan* [1979]. These waves are believed to play an important role in various plasma processes in the magnetosphere through wave-particle interactions. Examples of such processes include the diffusion of auroral electrons by electrostatic electron cyclotron waves [*Kennel and Ashour-Abdalla*, 1982], the generation of AKR through relativistic cyclotron resonance [*Gurnett*, 1974; *Wu and Lee*, 1979] and the acceleration and heating of ions and electrons by waves in the auroral region leading to the formation of ion and electron conical distributions (see, for example, *Chang et al.* [1986], *Crew et al.* [1990], *Lysak* [1986], *Temerin and Cravens* [1990], and *Wong et al.* [1988], among others).

The whistler mode has been studied extensively in the past, primarily due to the interest in VLF emissions, auroral hiss, and lightning-related phenomena. In the midaltitude polar magnetosphere, the electron plasma frequency $\omega_e = (4\pi n_e e^2/m_e)^{1/2}$ is typically less than the electron cyclotron frequency $\Omega_e = |e|B_o/m_e c$, where m_e is the electron rest mass, n_e is the electron density, B_o is the magnitude of the ambient magnetic field, and c is the speed of light. Under this condition, the whistler mode propagates between the lower hybrid frequency, which is approximately the ion plasma frequency ω_i, and ω_e. The frequently observed whistler mode auroral hiss is believed to be generated near the resonance cone either by precipitating electrons or by upward moving electron beams [*Gurnett et al.*, 1983]. The whistler waves excited near the resonance cone are quasi-electrostatic waves with negligible magnetic components; however, analysis of the "funnel-shaped" auroral hiss observed by DE 1 indicates that the auroral hiss has a considerable magnetic component [*Gurnett et al.*, 1983]. Subsequent stability analysis using the observed particle distributions has revealed that the electron acoustic wave, rather than the whistler wave, is the dominant unstable wave driven by such electron beam distributions [*Lin et al.*, 1984, 1985; *Tokar and Gary*, 1984]. The electron acoustic wave is electrostatic in nature, and thus might account for the electrostatic component of auroral hiss; however, the origin of the electromagnetic component of the hiss still remains unanswered.

In a different context, *Benson et al.* [1988] have reported ground-based detection of waves in the frequency range 150–300 kHz, indicating the generation of field-aligned waves in the auroral zone. The field-aligned waves observed by *Benson et al.* [1988] are electromagnetic and fall into the frequency range of the whistler mode and overlap the frequency range of AKR. However, because the theories usually proposed for the generation of AKR produce radiation in the extraordinary and ordinary modes which cannot reach the ground, the field-aligned radiation observed by *Benson et al.* [1988] must be generated by a different mechanism. Motivated by these observations, *Wu et al.* [1989] showed that an energetic electron population with either a temperature anisotropy or a trapped type distribution can generate field-aligned waves in the observed frequency range. More recently, *Ziebell et al.* [1991] have generalized *Wu et al.'s* [1989] theory to investigate propagation effects on the amplification of radiation along the field line.

Previously we have studied the generation of bursty radio emission by low-density anisotropic or gyrating electron beams [*Wong and Goldstein*, 1990] (hereinafter paper 1). In

Paper number 93JA02319.
0148-0227/94/93JA-02319$05.00

the present study we extend that analysis by including relativistic effects and show that the frequency range of the unstable waves excited by dense gyrating and/or anisotropic distributions can extend below Ω_e or even below ω_e. In this regard our analysis is a generalization of the previous work by *Wu et al.* [1989] because we extend into the relativistic regime, include oblique propagation, and use a more general distribution function that includes a beam component. The process we describe appears to provide an alternative to the cyclotron maser instability for generating *Z* and *O* mode radiation.

Physical Model and Results

The physical model we consider is the same as previously discussed in paper 1: a gyrating or anisotropic electron beam in a cold background magnetized plasma. Because the frequencies we consider are close to Ω_e or ω_e, we can ignore the ion contribution to the plasma dielectric. In paper 1 we discussed the conditions under which such distributions can arise and we do not repeat that discussion here. The general form of the energetic electron distribution we use is

$$f_b(u_\parallel, u_\perp) = \frac{A}{\pi^{3/2}\alpha_{\perp b}^2\alpha_{\parallel b}} \exp\left[-\frac{(u_\perp - u_{\perp 0})^2}{\alpha_{\perp b}^2} - \frac{(u_\parallel - u_b)^2}{\alpha_{\parallel b}^2}\right] \quad (1)$$

where $\mathbf{u} = \mathbf{p}/m_e$ is the momentum per unit mass, $\alpha_{\perp,\parallel b} = (2\kappa T_{\perp,\parallel b}/m_e)^{1/2}$, κ is Boltzmann's constant, u_b and $u_{\perp 0}$ are the momenta per unit mass of the electron beam parallel and perpendicular to the magnetic field, respectively, and the normalization constant is found from $A^{-1} = \exp(-u_{\perp 0}^2/\alpha_{\perp b}^2)[1 - i(u_{\perp 0}/\alpha_{\perp b})\, Z(i(u_{\perp 0}/\alpha_{\perp b})]$ to ensure that $\int d^3u f_b(\mathbf{u}) = 1$.

A general derivation of the relativistic electromagnetic dispersion equation for arbitrary directions of propagation can be found in the work by *Baldwin et al.* [1969]. In the appendix we give a brief description of how we solve the dispersion equation numerically. Most of the discussion below will be limited to parallel propagating solutions, primarily because the maximum growth is generally at 0°. However, we have also solved the more general obliquely propagating relativistic dispersion equation, and we discuss below some of those results (Figure 6).

For comparison purposes, we first show solutions to the nonrelativistic dispersion equation for parallel propagating modes excited by trapped electrons with energies of the order of several keV, a case discussed previously by *Wu et al.* [1989]. The dispersion relation was solved using $n_b = 0.9$, $n_e = 9n_c$, where n_b and n_c are the densities of the energetic and background electrons, respectively; and $n_e = n_b + n_c$. Note that, in contrast to paper 1, we emphasize here a regime in which the density of the energetic electron component, n_b, exceeds that of the background, n_c. We used five values of ω_e/Ω_e, viz. 0.1, 0.2, 0.4, 0.6, and 0.8. In the example shown in Figure 1, the drift of the electrons is zero, and the parallel and perpendicular temperatures of the energetic electrons are both 2.5 keV. The ring speed is $u_{\perp 0} = 2.0$ in units of $\alpha_{\perp b}$. In Figure 1 we plot the real and imaginary frequencies (ω_r and ω_i, respectively) as functions of wave number. The frequencies are normalized by Ω_e, and the wave numbers by Ω_e/c. Note that ω_r and ω_i are plotted on linear and logarithmic scales, respectively. One should keep in mind in these analyses that because the growth rates are functions of ω_e/Ω_e and n_b/n_e, specific values of density need not be specified.

As is evident from Figure 1, the instability exists for the entire range of the values of ω_e/Ω_e considered, as does the bandwidth of the instability. For small values of ω_e/Ω_e, the frequency of the unstable waves lies between ω_e and Ω_e, which is in the frequency regime of the *Z* and *O* modes. For larger values of ω_e/Ω_e, the frequency of the unstable waves can extend below ω_e; the waves are then in the whistler and *Z* mode branches for frequencies above the left-hand cutoff. This result is essentially the same as was found by *Wu et al.* [1989], as can be verified by comparing our Figure 1 with their Figure 3.

In Figure 2 we show the effect on the magnitude of the growth rates when using the relativistic dispersion relation. The parameters are the same as we used in Figure 1, except that now $\omega_e/\Omega_e = 0.8$. It is clear that both the bandwidth and magnitude of the instability are reduced. The reduction in bandwidth is from $\Delta kc/\Omega_e \cong 0.6$ to $\Delta kc/\Omega_e \cong 0.4$, while the maximum growth rate drops by nearly a factor of 5. Thus it is clear that relativistic effects can be quantitatively important in this class of instabilities. For the remainder of this paper, all results will be computed using the relativistic dispersion equation.

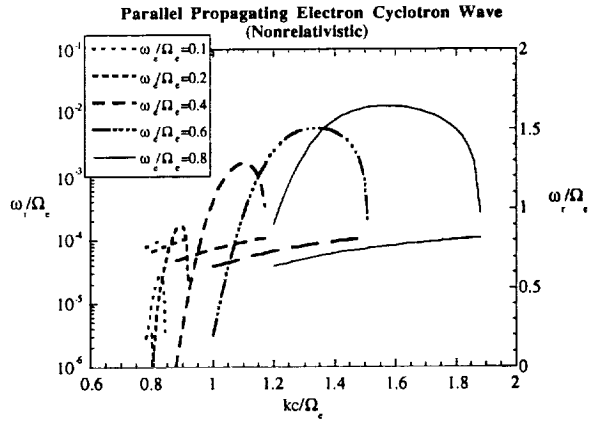

Figure 1. The unstable roots of the nonrelativistic dispersion equation plotted for comparison with Figure 3 of *Wu et al.* [1989]. The distribution function of the energetic electrons, given by (1), is normalized so that $n_b = 0.9$ and $n_e = 9n_c$. The parallel and perpendicular temperatures of the energetic electrons both equal 2.5 keV, and the ring speed is $u_{\perp 0}/\alpha_{\perp b} = 2.0$ (the beam speed $u_\parallel = 0$). The real and imaginary parts of ω are plotted on linear and logarithmic scales, respectively, for $\omega_e/\Omega_e = 0.1$, 0.2, 0.4, 0.6, and 0.8. Frequencies are normalized by Ω_e and wave numbers by Ω_e/c.

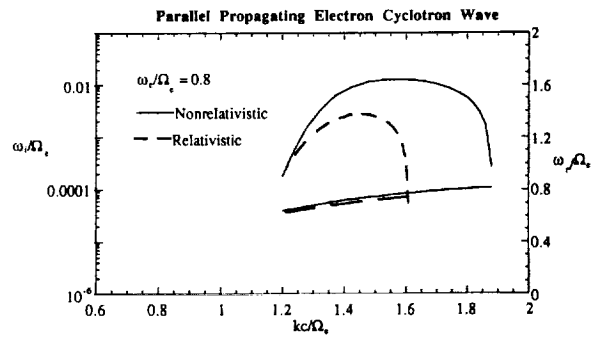

Figure 2. Comparison between solutions of the relativistic and nonrelativistic dispersion equations for the same parameters are were used in Figure 1 except that only the results for $\omega_e/\Omega_e = 0.8$ are shown.

For zero drift speed ($u_{\perp 0} = u_b = 0$), this instability can also be driven by a temperature anisotropy, as is illustrated in Figure 3. Here the density ratio between the energetic and background electron distributions remains as before, $\omega_e/\Omega_e = 0.6$, and the parallel temperature of the energetic electrons is kept constant at 2.5 keV, while the perpendicular temperature is increased from $T_{\perp b}/T_{\|b} = 4$ to $T_{\perp b}/T_{\|b} = 10$. For $T_{\perp b}/T_{\|b} = 4$ the growth rate is very small ($\omega_{i,max}/\Omega_e \cong 10^{-4}$), but it increases by more than 2 orders of magnitude as the anisotropy increases to $T_{\perp b}/T_{\|b} = 10$. Clearly, at $T_{\perp b}/T_{\|b} = 4$ the instability is near threshold (note the rapid increase from $T_{\perp b}/T_{\|b} = 4$ to $T_{\perp b}/T_{\|b} = 5$) — subsequent increases in $T_{\perp b}/T_{\|b}$ produce far smaller changes in the maximum rate of growth.

Figure 4 illustrates the behavior of the instability as the ring speed is varied from $u_{\perp 0}/\alpha_{\perp b} = 2.8$ to 3.2. The parameters used in these calculations are again the same as above, except that $\omega_e/\Omega_e = 0.4$. The growth rate is a fairly sensitive function of $u_{\perp 0}/\alpha_{\perp b}$, which can be understood because the free energy of the ring is equivalent to a temperature anisotropy, as discussed by *Wong and Goldstein* [1987]. Recall from Figure 2 that relativistic effects can significantly reduce the growth rate from the values calculated nonrelativistically, especially for relatively small values of ω_e/Ω_e and/or $u_{\perp 0}$. This must be kept in mind when comparing Figures 2 and 4 with the nonrelativistic calculation shown in Figure 1.

In Figure 5 we investigate how finite beam speed affects the instability as $u_b/\alpha_{\|b}$ is varied from 0 to 2. The parameters used are again as in Figure 1, except that $u_{\perp 0}/\alpha_{\perp b} = 2.5$ and $\omega_e/\Omega_e =$ 0.6. Small increases in $u_b/\alpha_{\|b}$ (from 0 to 1) cause the instability to broaden in bandwidth and to increase slightly in maximum growth. Further increase in $u_b/\alpha_{\|b}$ to 2 produces a reduction in growth and in bandwidth from what it was at $u_b/\alpha_{\|b} = 1$; however, it is still significantly broader than it was initially when $u_b/\alpha_{\|b} = 0$. This behavior contrasts sharply from the beam-driven radio emission discussed in paper 1 (cf. Figure 2 in that paper) in which the growth rate increased monotonically with increasing beam speed.

We have also investigated the behavior of this instability for oblique propagation. Again we take the thermal energy of the energetic electrons to be 2.5 keV, the density ratio of the energetic and cold components of the electron distribution equal to 9, the ring speed $u_{\perp 0}/\alpha_{\perp b} = 2.5$, and $\omega_e/\Omega_e = 0.6$. The distribution has no drift ($u_b = 0$). The real and imaginary parts of ω are plotted in Figure 6 as a function of θ, the angle between **k** and **B**. The plot is constructed at the wave number of maximum growth of the instability at $\theta = 0°$, $kc/\Omega_e = 1.28$. For this wave number, the instability extends to approximately 10°, and then drops rapidly to zero. This does not necessarily mean, however, that there is no instability at larger angles. For the parameters of this example, as the propagation angle changes, the wave number of local maximum growth at that value of θ shifts to lower values of k, and the cone of unstable wave vectors extends somewhat beyond 15°. Nonetheless, the instability still grows most rapidly at $\theta = 0°$. There is little Landau damping at these frequencies, and these oblique waves are primarily electromagnetic in nature.

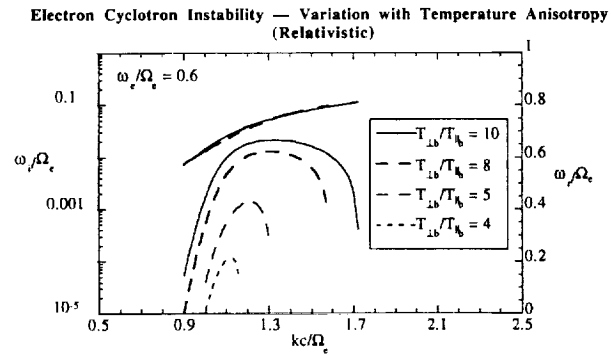

Figure 3. Variation in the growth rate of the electron cyclotron instability with changes in temperature anisotropy. The beam speed is 0, and $\omega_e/\Omega_e = 0.6$. The temperature anisotropy varies from $T_{\perp b}/T_{\|b} = 4$ to $T_{\perp b}/T_{\|b} = 10$. At $T_{\perp b}/T_{\|b} =$ 4 the instability is near threshold.

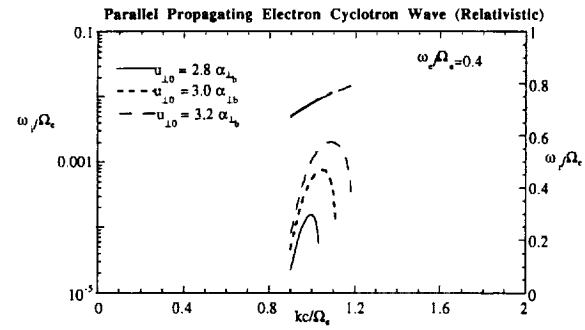

Figure 4. Variation in the growth rate of the instability for $\omega_e/\Omega_e = 0.4$ as the ring speed is varied from $u_{\perp 0}/\alpha_{\perp b} = 2.8$ to 3.2. All other parameters are the same as were used in Figure 1.

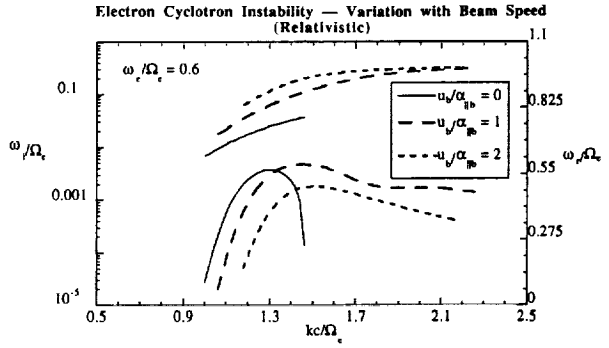

Figure 5. The effect of finite beam speed on the instability. In this case, $u_b/\alpha_{\|b}$ is varied from 0 to 2; $u_{\perp 0}/\alpha_{\perp b} = 2.5$, and $\omega_e/\Omega_e = 0.6$. All other parameters are the same as were used in Figure 1.

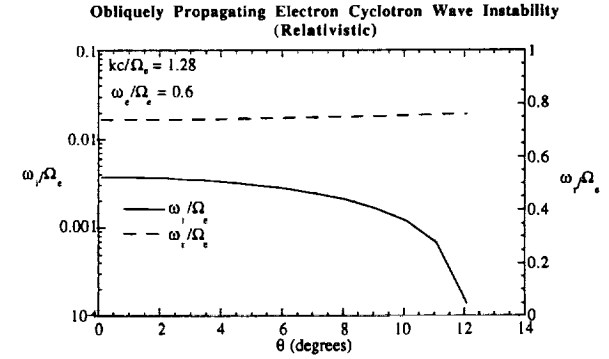

Figure 6. The behavior of the instability for off-angle propagation. The thermal energy is again 2.5 keV, $u_{\perp 0}/\alpha_{\perp b} =$ 2.5, and $\omega_e/\Omega_e = 0.6$. The beam drift speed $u_{\|b} = 0$, and $kc/\Omega_e =$ 1.28. The density of the beam is the same as was used in all figures above.

As the value of ω_e/Ω_e increases, e.g., $\omega_e/\Omega_e = 0.8$, the situation changes significantly. For large values of ω_e/Ω_e, maximum growth occurs at oblique propagation and at larger values of k than for the local maximum at $\theta = 0°$. We suspect that this change in the nature of the solution arises from the fact that the real part of the wave frequency is above the electron plasma frequency when the ratio ω_e/Ω_e is small, whereas when $\omega_e/\Omega_e = 0.8$, the excited wave has a frequency below ω_e (*cf.* Figure 1). Thus at large values of ω_e/Ω_e, the excited wave can be in the Z and whistler modes, while for small values of ω_e/Ω_e, the wave can only propagate in the Z and O modes (for a discussion of which wave modes exist at particular frequencies in the auroral region, see Figure 5 of *Gurnett et al.* [1983]). This behavior of the instability with changing ω_e/Ω_e suggests that the trapped (or ring) distribution is an effective population for generating whistler waves if the physical parameters are appropriate.

Discussion

The fundamental result of this calculation is the demonstration that a temperature anisotropy or a ring-beam electron distribution can generate electron cyclotron waves with frequencies that extend from below to above ω_e, but still below Ω_e for an underdense plasma. The calculation is relativistic and allows for arbitrary direction of propagation. Previous work [*Wu et al.*, 1989] was confined to parallel propagation and was a nonrelativistic calculation. Our result for parallel propagation agrees qualitatively with Wu et al.'s results; however, as shown in Figure 2, the effect of the relativistic corrections to the dispersion equation is to reduce substantially both the magnitude of the growth rate and the bandwidth of the unstable waves.

We also investigated the effect that finite beam speed has on the instability, an effect not considered previously. For small beam speeds, the growth rates can be enhanced and the bandwidths broadened. But as the beam speed increases, the growth rate decreases (cf. Figure 5). In paper 1 we studied the generation of bursty radio emission and showed that in plasma regimes in which $\omega_e/\Omega_e < 1$, anisotropic electron beams, or gyrating electron beams, can excite directly right-hand polarized broadband electromagnetic radiation in the X mode. The present analysis extends that work to waves with frequencies below Ω_e and also includes relativistic effects in the dispersion equation. In addition, the mechanism described in paper 1 generated unstable X mode waves when the electron distributions had large drift speeds. In contrast, for the parameters used here, the present mechanism is suppressed for large electron drift speeds and excites waves primarily in the Z or O mode. Nonetheless, the free energy source in both situations is the temperature anisotropy or ring component of the energetic electrons (the present mechanism operates even in the absence of any drift).

Recently, *Winglee et al.* [1992] have performed a one-dimensional (with three components of velocity), relativistic electromagnetic particle simulation that showed that an anisotropic electron distribution can generate freely propagating right-hand circularly polarized electromagnetic radiation if the beam speed is sufficiently large—in agreement with the results of paper 1. Winglee et al.'s simulations are periodic, and the wave vectors are parallel to the magnetic field. Besides the freely propagating wave, *Winglee et al.* [1992] also found an instability with frequencies below Ω_e—a result consistent with the theoretical analysis here. For lower values of the beam speed they found that the dominant wave mode consisted of waves with frequencies $\omega_r < \Omega_e$, whereas for large beam speeds, the dominant mode was the freely propagating X mode, also in agreement with the results shown here and in paper 1.

The motivation for the present work was observations of Z mode radiation in the Earth's auroral zone [*Gurnett et al.*, 1983] and similar phenomena at other planets [*Gurnett et al.*, 1990; *Kurth and Gurnett*, 1991]. Although Z mode radiation can be generated by the cyclotron maser instability (see, for example, *Hewitt et al.* [1983]), ray tracing studies [*Menietti and Lin*, 1986] indicate that cyclotron maser resonance may not be the only mechanism responsible for the observed Z mode emission because the generation and subsequent refraction of the waves do not appear consistent with observations. Electron cyclotron waves generated by temperature anisotropies or ring-beam distributions can have frequencies between ω_e and Ω_e in the Z and O mode ranges. Because the waves are mostly right-hand polarized, we suspect that this mechanism mainly produces Z mode radiation. The electron cyclotron waves excited in this frequency range are predominantly field-aligned and have a much broader bandwidth in frequency than waves generated by the cyclotron maser instability. Thus the electron cyclotron wave generation mechanism discussed here may provide another, complementary, explanation for observed Z mode radiation. Because a ring-beam distribution is also capable of generating Z mode radiation via the cyclotron maser instability, determining which mechanism actually dominates in any specific situation requires detailed modeling that is beyond the scope of this paper.

Conclusions

We have examined the role of relativistic effects on the generation of electron cyclotron radiation by anisotropic energetic electrons. The anisotropies are assumed to be due to either temperature anisotropies or ring (trapped) distributions. Although our results are qualitatively in agreement with previous work [*Wu et al.*, 1989], relativistic effects tend to suppress significantly the growth rate. We have also found it possible to excite electromagnetic whistler waves with maximum growth at a substantial angle from the background field for large values of ω_e/Ω_e (~ 0.8, but still less than unity). The excitation mechanism discussed in this paper may provide an alternative explanation to the cyclotron maser instability for the generation of Z mode radiation observed in planetary magnetospheres.

As shown in paper 1 and in the simulations of *Winglee et al.* [1992], a gyrating or anisotropic electron distribution can excite a variety of waves in several different frequency ranges. In addition, the same class of distributions is also unstable to the cyclotron maser instability. Which mechanism (or wave mode) dominates will depend on the detailed form of distribution and on details of the background plasma parameters. A comprehensive comparison of the relative importance of these mechanisms will have to await more extensive analytic work coupled with two-dimensional numerical simulations, including a study of the convective properties of these instabilities along auroral field lines (for example, *Ziebell et al.* [1991]).

Appendix

In this derivation, two electron components are immersed in a uniform, external magnetic field $\mathbf{B} = B_o \hat{e}_z$: a low-energy thermal background and an energetic relativistic population. The density ratio between these two populations can be arbitrary. Because our interest is confined to waves with frequencies of the order of the electron cyclotron frequency, which is much greater than the ion plasma frequency, ion dynamics can

be neglected. Consequently, the dispersion equation of the linearized Vlasov-Maxwell equations can be written in the form [*Wong et al.*, 1989]

$$\mathbf{D}(\mathbf{k},\omega)=\left(1-\frac{k^2c^2}{\omega^2}\right)\mathbf{I}+\frac{c^2}{\omega^2}\mathbf{kk}+\sum_{\alpha}\mathbf{Q}^{\alpha}(\mathbf{k},\omega)=0 \qquad \text{(A1)}$$

where

$$\mathbf{Q}^{\alpha}(\mathbf{k},\omega)=2\pi\frac{\omega_{\alpha}^2}{\omega^2}\int_{-\infty}^{+\infty}du_{\parallel}\int_{0}^{\infty}du_{\perp}\frac{u_{\parallel}}{\gamma}\left(u_{\perp}\frac{\partial}{\partial u_{\parallel}}-u_{\parallel}\frac{\partial}{\partial u_{\perp}}\right)F_{\alpha}\hat{e}_z\hat{e}_z$$
$$+2\pi\frac{\omega_{\alpha}^2}{\omega^2}\int_{-\infty}^{+\infty}du_{\parallel}\int_{0}^{\infty}du_{\perp}\left[\omega\frac{\partial}{\partial u_{\perp}}+\frac{k_{\parallel}}{\gamma}\left(u_{\perp}\frac{\partial}{\partial u_{\parallel}}-u_{\parallel}\frac{\partial}{\partial u_{\perp}}\right)\right]F_{\alpha}$$
$$\times\sum_{n=-\infty}^{n=+\infty}\frac{\mathbf{T}^n}{\gamma\omega-n\Omega_e-k_{\parallel}u_{\parallel}} \qquad \text{(A2)}$$

where $\gamma=(1+u^2/c^2)^{1/2}$, and $\alpha=b,e$ refers to the background and energetic electrons, respectively. The wave vector $\mathbf{k}$ is assumed to lie in the x-z plane so that $\mathbf{k}=k_{\perp}\hat{e}_x+k_{\parallel}\hat{e}_z$; $\mathbf{I}$ is the unit dyadic; $\omega_{\alpha}^2=4\pi n_{\alpha}e^2/m_{\alpha}$; $\mathbf{u}$ is the momentum per unit mass and is given by $\mathbf{u}=\mathbf{p}/m_e$; and n_{α} is the number density of species α. The tensor $\mathbf{T}^n$ is defined by

$$\mathbf{T}^n=\begin{bmatrix}\frac{n^2\Omega_e^2}{k_{\perp}^2}J_n^2 & -\frac{in\Omega_e}{k_{\perp}}u_{\perp}J_nJ_n' & \frac{n\Omega_e}{k_{\perp}}u_{\parallel}J_n^2\\ \frac{in\Omega_e}{k_{\perp}}u_{\perp}J_nJ_n' & u_{\perp}^2J_n'^2 & iu_{\parallel}u_{\perp}J_nJ_n'\\ \frac{n\Omega_e}{k_{\perp}}u_{\parallel}J_n^2 & -iu_{\parallel}u_{\perp}J_nJ_n' & u_{\parallel}^2J_n^2\end{bmatrix} \qquad \text{(A3)}$$

where $J_n=J_n(k_{\perp}u_{\perp}/\Omega_e)$.

The method for obtaining numerical solutions to the relativistic dispersion equation is cumbersome, and here we only outline the approach employed in reaching the solutions given above. The relativistic factor γ is expanded to $O(u^4/c^4)$, except for the resonant denominator in which we keep the entire expression $\gamma\omega-n\Omega_e-k_{\parallel}u_{\parallel}$. One then integrates over $u_{\parallel}$ analytically and writes the resulting expression in terms of the plasma dispersion function (the Z function defined by *Fried and Conte* [1961]). In contrast to nonrelativistic calculations, the argument of the Z function now depends on $u_{\perp}$ because of the factor of γ, which appears in the resonance condition. The remaining integration over $u_{\perp}$ is performed numerically using a standard root-finding algorithm to compute (complex) ω.

Acknowledgments. H.K.W. would like to thank D. Menietti for valuable discussions. This work was supported in part by the Space Physics Theory Program at the Goddard Space Flight Center and NASA grants NAGW-2412 (Neptune Data Analysis Program) and NAGW-1620 to the Southwest Research Institute.

The Editor thanks L.-C. Lee and M. A. Temerin for their assistance in evaluating this paper.

References

Baldwin, D. E., I. B. Bernstein, and M. P. H. Weenink, Kinetic theory of plasma waves in a magnetic field, in *Advances in Plasma Physics*, edited by A. Simon and W. B. Thompson, p. 1, Wiley-Interscience, New York, 1969.

Benson, R. F., M. D. Desch, R. D. Hunsucker, and J. G. Romick, Ground-level detection of low- and medium-frequency auroral emissions, *J. Geophys. Res.*, *93*, 277, 1988.

Chang, T., G. B. Crew, N. Hershkowitz, J. R. Jasperse, J. M. Retterer, and J. D. Winningham, Transverse acceleration of oxygen ions by electromagnetic ion cyclotron resonance with broad band left-hand polarized waves, *Geophys. Res. Lett.*, *13*, 636, 1986.

Crew, G. B., T. Chang, J. M. Retterer, W. K. Peterson, D. A. Gurnett, and R. L. Huff, Ion cyclotron resonance heated conics: Theory and observations, *J. Geophys. Res.*, *95*, 3959, 1990.

Fried, B. D., and S. D. Conte, *The Plasma Dispersion Function*, Academic, San Diego, Calif., 1961.

Gurnett, D. A., W. S. Kurth, I. H. Cairns, and L. J. Granroth, Whistlers in Neptune's magnetosphere: Evidence of atmospheric lightning, *J. Geophys. Res.*, *95*, 20,967, 1990.

Gurnett, D. A., The Earth as a radio source: Terrestrial kilometric radiation, *J. Geophys. Res.*, *79*, 4227, 1974.

Gurnett, D. A., S. D. Shawhan, and R. R. Shaw, Auroral hiss, Z mode radiation, and auroral kilometric radiation in the polar magnetosphere: DE 1 observations, *J. Geophys. Res.*, *88*, 329, 1983.

Hewitt, R. G., D. B. Melrose, and G. A. Dulk, Cyclotron maser emission of auroral Z mode radiation, *J. Geophys. Res.*, *88*, 10,065, 1983.

Kennel, C. F., and M. Ashour-Abdalla, Electrostatic waves and the strong diffusion of magnetospheric electrons, in *Magnetospheric Plasma Physics*, edited by A. Nishida, p. 245, D. Reidel, Hingham, Mass., 1982.

Kurth, W. S., and D. A. Gurnett, Plasma waves in planetary magnetospheres, *J. Geophys. Res.*, *96*, 18,977, 1991.

Lin, C. S., J. L. Burch, S. D. Shawhan, and D. A. Gurnett, Correlation of auroral hiss and upward electron beams near the polar cusp, *J. Geophys. Res.*, *89*, 925, 1984.

Lin, C. S., D. Winske, and R. L. Tokar, Simulation of the electron acoustic instability in the polar cusp, *J. Geophys. Res.*, *90*, 8269, 1985.

Lysak, R. L., Ion acceleration by wave-particles interactions, in *Ion acceleration in the magnetosphere and ionosphere*, *Geophys. Monogr. Ser.*, vol. 38, edited by T. Chang, M. K. Hudson, J. R. Jasperse, R. G. Johnson, P. M. Kintner, M. Schulz and G. B. Crew, p. 261, AGU, Washington, D. C., 1986.

Menietti, J. D., and C. S. Lin, Ray tracing survey of Z mode emissions from source regions in the high-altitude auroral zone, *J. Geophys. Res.*, *91*, 13,559, 1986.

Shawhan, S. D., Magnetospheric plasma waves, in *Solar System Plasma Physics*, edited by C. F. Kennel and E. N. Parker, North-Holland, Amsterdam, 1979.

Temerin, M. A., and D. Cravens, Production of electron conics by stochastic acceleration parallel to the magnetic field, *J. Geophys. Res.*, *95*, 4285, 1990.

Tokar, R. L., and S. P. Gary, Electrostatic hiss and the beam-driven electron acoustic instability in the dayside polar cusp, *Geophys. Res. Lett.*, *11*, 1180, 1984.

Winglee, R. M., J. D. Menietti, and H. K. Wong, Numerical simulations of bursty radio emissions from planetary magnetospheres, *J. Geophys. Res.*, *97*, 17,131, 1992.

Wong, H. K., and M. L. Goldstein, Proton beam generation of whistler waves in the Earth's foreshock, *J. Geophys. Res.*, *92*, 12,419, 1987.

Wong, H. K., and M. L. Goldstein, A mechanism for bursty radio emission in planetary magnetospheres, *Geophys. Res. Lett.*, *17*, 2229, 1990.

Wong, H. K., J. D. Menietti, C. S. Lin, and J. L. Burch, Generation of electron conical distributions by upper hybrid waves in the Earth's solar region, *J. Geophys. Res.*, *93*, 20,025, 1988.

Wong, H. K., D. Krauss-Varban, and C. S. Wu, On the role of the energy of suprathermal electrons in the generation of auroral kilometric radiation, *J. Geophys. Res.*, *94*, 5327, 1989.

Wu, C. S., and L. C. Lee, A theory of terrestrial kilometric radiation, *Astrophys. J.*, *230*, 621, 1979.

Wu, C. S., P. H. Yoon, and H. P. Freund, A theory of electron cyclotron waves generated along auroral field lines observed by ground facilities, *Geophys. Res. Lett.*, *16*, 1461, 1989.

Ziebell, L. F., C. S. Wu, and P. H. Yoon, Kilometric radio waves generated along auroral field lines observed by ground facilities: A theoretical model, *J. Geophys. Res.*, *96*, 1495, 1991.

H. K. Wong, Department of Space Sciences, Southwest Research Institute, San Antonio, TX 78284.

M. L. Goldstein, Laboratory for Extraterrestrial Physics, Code 692, NASA Goddard Space Flight Center, Greenbelt, MD 20771.

(Received May 18, 1993; revised August 9, 1993; accepted August 13, 1993.)

Electromagnetic Hiss and Lower Hybrid Waves in the Polar Magnetosphere

H K Wong (Department of Space Sciences, Southwest Research Institute, San Antonio, TX 78228-0510; 210-522-3627; kit@swri.space.swri.edu)

J D Menietti (Department of Physics and Astronomy, University of Iowa, Iowa City, IA 52242)

C S Lin (Auroral Science Inc., 4502 Centerview Dr., Suite 215, San Antonio, TX 78228)

Electromagnetic waves with frequencies indicative of whistlers and lower hybrid waves are frequently observed by DE-1 in the Earth's auroral region. These waves are typically observed outside the region and at the higher magnetic field side of intense electron precipitation. Comparison of the electric and magnetic field spectrum indicates that these waves are predominately magnetic and the refractive indices are much larger than unity except when the wave frequencies are very close to the local lower hybrid frequency. It is suggested that these electromagnetic waves can be explained by waves generated near the resonance cone and propagate away from the source. The role that these electromagnetic waves can play in particle acceleration processes at low altitude will be discussed.

1. 1994 Spring Meeting

2. 003825915

3. (a) H K Wong
   Div 15
   Southwest Research Institute
   San Antonio, TX 78228

   (b) Tel: 210-522-3627

   (c) fax: 210-647-4325

4. SM

5. (a)
   (b) 2772 Plasma waves and instabilities
   7867 Wave-particle interactions
   2704 Auroral phenomena

6. Oral session preferred

7. 30% at 1992 Spring Meeting

8. $50 Check enclosed

9. C

10. None

11. No